Supplementary information for:

Charge Transfer Excitons in a Donor-Acceptor Amphidynamic Crystal: the Role of Dipole Orientational Order

Joshua Macdonald[1], Giacomo Piana[2], Massimiliano Comin,[3] Elizabeth von Hauff [4], Gabriele Kociok-Köhn[5], Chris Bowen[6], Pavlos Lagoudakis[2,7], Gabriele D'Avino[3], Enrico Da Como[1]**

[1] Centre for Photonics and Photonic Materials (CPPM) and Department of Physics, University of Bath, Claverton Down, Bath BA2 7AY, UK

[2]Physics and Astronomy, University of Southampton, University Road, Southampton SO17 1BJ, UK

[3]Institut Néel CNRS and Université Grenoble Alpes, F-38042 Grenoble, France

[4]Department of Physics and Astronomy, Vrije Universiteit, de Boelelaan 1081, 1081 HV Amsterdam, Netherlands

[5]Material and Chemical Characterization Facility, University of Bath, Claverton Down, Bath BA2 7AY, UK

[6]Department of Mechanical Engineering, University of Bath, Claverton Down, Bath BA2 7AY, UK

[7]Skolkovo Institute of Science and Technology (Skoltech), Skolkovo, Moscow 121205, Russia

Email: e.da.como@bath.ac.uk; j.w.r.macdonald@bath.ac.uk

Experimental

Crystal Growth technique

Crystal growth was carried out following the technique described in Henderson et al.,[1] pictured in figure S1. Physical vapor transport was used to grow the perylene-TBPA co-crystals in a horizontal quartz tube with argon flow. Perylene and TBPA were purified by sublimation and placed in the tube and the tube placed into the furnace such that perylene and TBPA were at the high-temperature end of the furnace. During the growth procedure, the perylene and TBPA was sublimated and carried by argon flowing at 130 cm^3/minute to the cool end of the furnace. The temperature for the hot, middle and cold zone of the furnace were set to 231, 187 and 147 °C respectively for 12 hours of growth time. Needle-shaped crystals with a maximum length of 15 mm and width of 2 mm were deposited midway through the tube and collected once the system

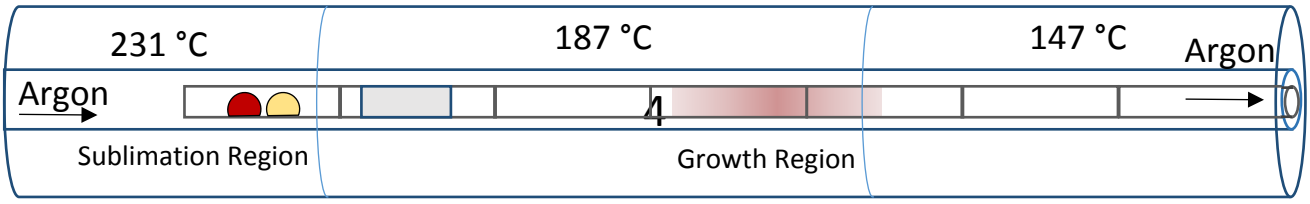

Figure S1. Illustration of cocrystal growth procedure in a horizontal quartz tube placed in a furnace with temperatures set as labelled.

had cooled.

X-ray Diffraction

A suitable single crystal for data collection was mounted on a Dual-Thickness MicroMount™ unoriented polymer with a drop of fomblin® perfluoro polyether oil. A variable temperature data collection at 290K and 150K was setup. Prior to each measurement the crystal was rotated by 360 degrees in 6 degree increments and 60 images were taken to detect any changes or slippage of the crystal. Intensity data were collected on a Rigaku Supernova Dual, EosS2 system using monochromated Cu-Kα radiation (λ = 1.54184 Å). Unit cell determination, data collection and data reduction were performed using the CrysAlisPro software. An empirical absorption correction using spherical harmonics and a numerical absorption correction based on gaussian integration over a multifaceted crystal model was employed. The structure was solved with SHELXT and refined by a full-matrix least-squares procedure based on F^2 (SHELXL-2018/3) [2]. All non-hydrogen atoms were refined anisotropically. Hydrogen atoms were placed onto calculated positions and refined using a riding model.

Reflectivity

Reflectivity measurements were obtained using a Cary 5000 UV-Vis-NIR spectrophotometer custom modified for temperature. The crystal was mounted in an Oxford Instruments Microstat He cryostat with quartz sapphire windows and the temperature was controlled using liquid nitrogen and an Oxford Instruments ITC503 temperature controller. A reference spectrum was gathered using a silver mirror and subtracted from the data using the Cary WinUV software to account for the emission spectrum and detection sensitivity of the spectrophotometer. Realignment of the sample was carried out between each measurement to obtain maximum signal and compensate for any movement of the crystal due to the change in temperature.

Kramers-Kronig Transform

RefFIT software was used in agreement with the procedure in Kuzmenko, 2005 [3] to transform the measured reflectivity data into an approximation of the absorption of perylene-TBPA using the dielectric function. The imaginary part of the dielectric function is able to provide information on the absorption spectrum, as the absorption coefficient, α, can be related to ε'' by

$$\alpha(\omega) = \frac{\omega\varepsilon''(\omega)}{c_0 n(\omega)},$$

where ω is the angular frequency, c_0 is the speed of light in vacuum and $n(\omega)$ is the refractive index [4]. This transform was obtained by assigning Lorentzian oscillators to the peaks and features observed in the reflectivity spectra to construct a mathematical approximation of the spectra. The values of the transverse frequency, plasma frequency and linewidth for each Lorentzian as well as the value of epsilon at infinity were adjusted both manually and using a built-in fitting algorithm until adequate, physically appropriate fits to the reflectivity spectra were obtained.

Photoluminescence Measurements

For PL, the optical excitation was obtained with a laser light having an energy density of 100 nJ/cm^2 (5 MHz repetition rate and 350 nW laser power) and wavelength of 420 nm provided by supercontinuum white laser (Fianium WhiteLase) monochromated with a tunable bandpass transmission filter (Fianium SuperChrome). The sample was mounted in a closed-loop He cryostat and its temperature was controlled through an Oxford Instruments ITC503 unit. The PL was collected and recorded by a fibre-coupled spectrometer (BWTek Glacier X).

Theoretical modelling

The Hamiltonian of the D_1AD_2 trimer is defined on the basis of the states in figure 5a as follows:

$$H = \sum_{i=1,2} \left[\varepsilon_i \, |i\rangle\langle i| - t_i(|0\rangle\langle i| + |i\rangle\langle 0|) \right]$$

where $\varepsilon_i = \Delta_{DA} - \frac{1}{\varepsilon_r r_i} + e(\phi_{Di} - \phi_A)$, with: Δ_{DA} the difference between the D ionization potential and the A electron affinity; ε_r the relative dielectric constant; r_i the distance between molecular centroids of D_i and A; e the electron charge; ϕ_{Di} (ϕ_A) the electrostatic potential generated by TBPA dipoles at D_i (A) molecular centroid; t_i the intermolecular CT coupling. The non-zero elements of the dipole moment operator are $\mu_{11} = e\, r_1$ and $\mu_{22} = e\, r_2$. Our calculations fix Δ_{DA}=3 eV, ε_r=3, and determine other quantities either from structural x-ray data or from explicit calculations. $t_i = \sqrt{2}\langle \varphi_{Di} | F_{ADi} | \varphi_A \rangle$ are calculated at density functional theory (PBE0 /def2-SVP) level, being φ_{Di} (φ_A) the HOMO (LUMO) of D_i (A), and F_{ADi} the Fock operator of the AD_i dimer.

Electrostatic calculations explicitly considered the cell parameters and molecular positions of the x-ray LPT or HTP structure. The TBPA molecule has been described as an extended dipole (two charges $q = \pm \mu/d$, with dipole $\mu =$ 4.5 Debye, dipole length d=3 Å),[5] higher multipole moments of TBPA or perylene molecules were not accounted for in the modelling. Periodic boundary conditions were implemented by considering interactions with periodic replica within a distance of 10 nm, ensuring a convergence < 0.1 meV per DA pair on total energies. Table S1 reports electrostatic site potentials and intermolecular CT couplings calculated for the LTP and HTP.

Electrostatic calculations of disordered samples of the HTP were performed on a 2x3x3 supercell. Because of the two possible antiparallel orientations of each of the 18 TBPA molecules in the

supercell, the phase space for this system counts 2^{18}= 262144 configurations. This large configurational space has been sampled with 10000 configurations generated by randomly assigning one of the two equiprobable orientations to each TBPA molecule. The total energy and the absorption spectrum (averaged over all trimers in sample) of each configuration are calculated. The absorption spectra at finite temperature are then calculated as a Boltzmann average. The distribution of energies of the sampled microscopic configurations is shown in Figure S2. We have verified that the DOS in Figure S2 and the absorption spectra in Figure 5d of the main text can be accurately calculated with any random subset of 2000 of the 10000 sampled configurations. This ensures that the properties of interest are converged with respect to the phase space sampling.

The effect of a single TBPA orientational defect on the absorption spectrum of the HTP is addressed in Figure S3. The most intense peak of the 300 K absorption can be ascribed to the defect free structure, while the others to thermally accessible disordered structures with orientational defects placed in the close proximity of the region of interest for CTE (the central DAD trimer).

The model presented above strictly describes CT transitions polarized parallel to the stack axis. Absorption of light polarized perpendicular to the stack may result either from CT transition between molecules belonging to different stacks, or from considering the actual molecular size, i.e. upon going-beyond the point-molecule approximation inherent to the model. These two hypotheses are addressed in the following.

Within the Mulliken model, the absorption intensity of CT transitions is proportional to the square of the CT coupling. We have hence computed intra- and inter-stack CT couplings between TBPA and neighbouring perylene molecules, see Figure S4. The data reported in Table S2, show that

intra-stack couplings are much larger than inter-stack ones. The absorption cross section for CT transitions between molecules of different stacks in hence expected to be 2-3 orders of magnitude smaller than that polarized along the stack.

In second instance, we have considered the actual molecular size and shape, by computing the excitations at TD-DFT level for perylene-TBA dimer (DA) and trimers (DAD and ADA) extracted from the LTP crystal structure. In all cases, the lowest-energy excitation is a pure HOMO-LUMO transition from perylene to TBPA. The components of the transition dipole moment of this excitation, reported in Table S3, show that about 90% of the absorption intensity is polarized parallel to the stack axis.

Table S1. Microscopic parameters (in meV), intermolecular CT couplings and electrostatic site potentials, entering the trimer model for optical excitations. HTP data refer to the hypothetical disorder-free structure.

	t_1	t_2	ϕ_{D1}	ϕ_{D2}	ϕ_A
LTP	267	229	409	106	257
HTP	190	142	32	-32	0

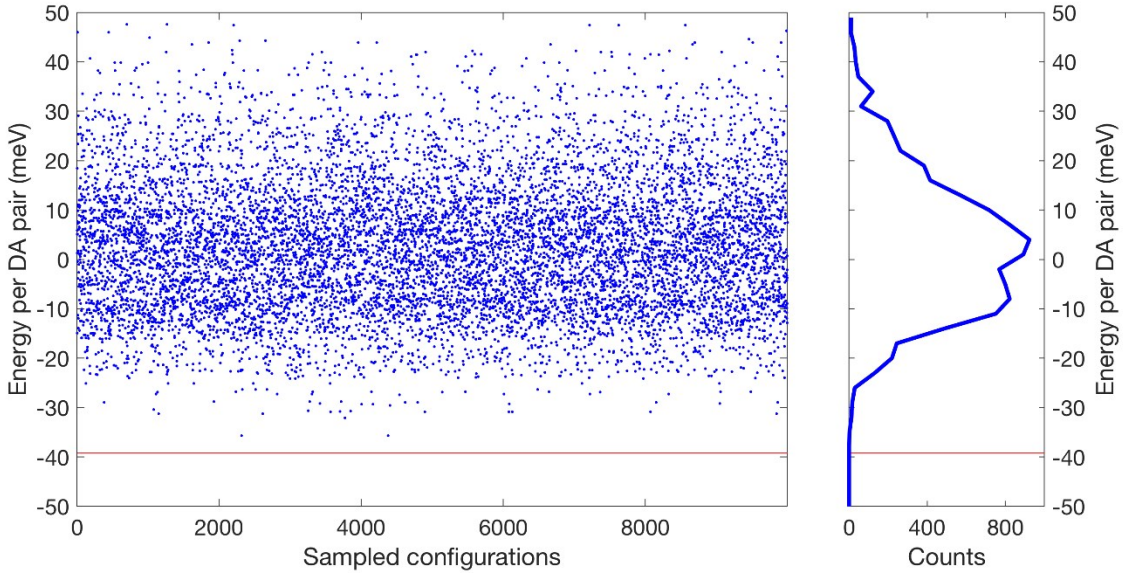

Figure S2. Energies of the sampled disordered configurations of the HTP (left) and the corresponding distribution (right). Dipolar interactions determine a spread of energies per DA pair over a 100 meV range. The red line marks the energy of the disorder free HTP structure. Lowest-energy disordered configurations are with 3 meV from the disorder free one, largely contributing to the absorption spectrum at finite temperature.

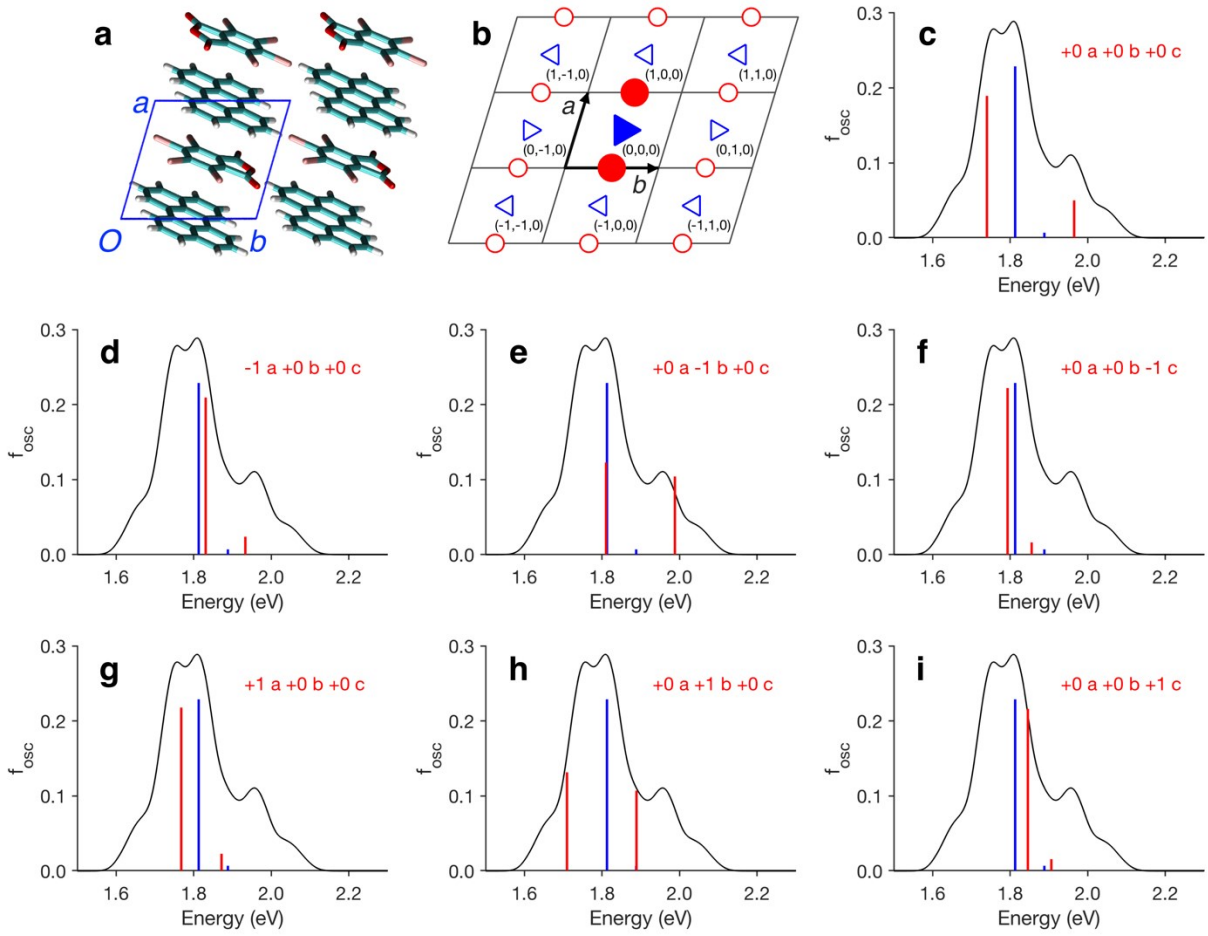

Figure S3. Absorption spectra of the HTP in the presence of a single TBPA orientational defect. (a) Defect free HTP crystal structure and (b) its simplified sketch, showing the DAD trimer considered in the calculation of the absorption spectrum (filled symbols), and TBPA molecules in the neighbouring cells (triangles with different orientations, mimicking dipolar directions). The number between parentheses label TBPA sites, where a defect can be created by flipping the corresponding dipole. (c-i) Absorption spectra calculated for a single orientational defect placed at the TBPA site indicated in each panel (red bars). Blue bars correspond to the excitations in the disorder free structure, the black line is the absorption spectrum at 300 K.

Table S2: intermolecular CT couplings (meV units) between TBPA and perylene molecules in the LTP structure. Labels A-F identify molecular dimers, see Figure S4. Intra-stack couplings (A,B) are much larger than intra-stack ones (C-F).

t_A	t_B	t_C	t_D	t_E	t_F
229	267	<1	2	4	6

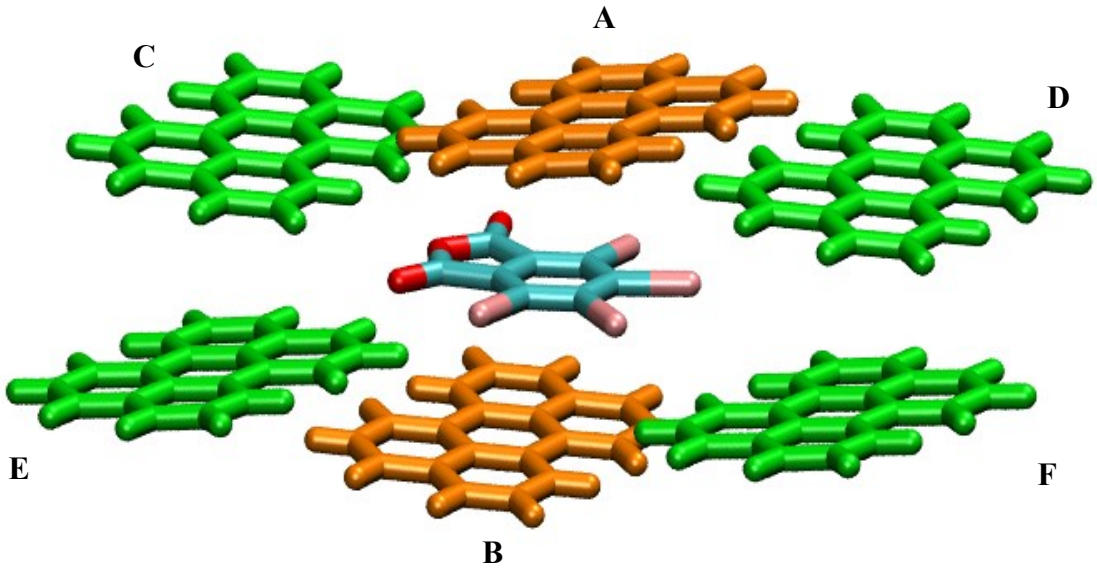

Figure S4: view of a TBPA molecule and the neighboring perylenes in the LTP crystal structure. Perylene neighbors within the stack are displayed in orange, those in other stacks in green. Molecular labels A-F are assigned to identify transfer integral between the central TBPA and each perylene (see Table S3).

Table S3: Squared transition dipole moment of the lowest-energy CT transition in perylene-TBPA dimers and trimers calculated at TD-PBE0/def2-SVP level. The components parallel and perpendicular to the stack are reported.

system	$\lvert\mu_{tr}\rvert^2$	$\lvert\mu_{tr}^{\parallel}\rvert^2$	$\lvert\mu_{tr}^{\perp}\rvert^2$
DA	0.378	0.330	0.048
DAD	0.826	0.778	0.048
ADA	0.812	0.736	0.076

Unit Cell Parameters

Table S4 Unit cell parameters obtained by x-ray diffraction of perylene-TBPA in its high temperature phase (at 290 K) and low temperature phase (at 150 K)

Temperature	***290 K***	***150 K***
Crystal system	*Triclinic*	*Triclinic*
Space group	*P-1*	*P-1*
a	*7.7182(4) Å*	*9.9529(5) Å*
b	*9.1941(6) Å*	*10.0251(4) Å*
c	*9.1951(6) Å*	*12.5133(6) Å*
α	*66.644(6) °*	*85.623(4) °*
β	*73.063(5) °*	*73.770(4) °*
γ	*84.331(5) °*	*68.865(4) °*
Volume	*572.95(7) Å^3*	*1117.75(10) Å^3*

References

1. Henderson, J.; Masino, M.; Hatcher, L. E.; Kociok-Kohn, G.; Salzillo, T.; Brillante, A.; Raithby, P. R.; Girlando, A.; Da Como, E., New Polymorphs of Perylene:Tetracyanoquinodimethane Charge Transfer Cocrystals. *Cryst. Growth Des.* **2018,** *18* (4), 2003-2009.
2. Sheldrick, G., Crystal structure refinement with SHELXL. *Acta Crystallographica Section C* **2015,** *71* (1), 3-8.
3. Kuzmenko, A. B., Kramers–Kronig constrained variational analysis of optical spectra. *Review of Scientific Instruments* **2005,** *76* (8), 083108.
4. Kuzmany, H., *Solid-State Spectroscopy: An Introduction*. Springer: Heidelberg, 1998.
5. Harada, J.; Ohtani, M.; Takahashi, Y.; Inabe, T., Molecular Motion, Dielectric Response, and Phase Transition of Charge-Transfer Crystals: Acquired Dynamic and Dielectric Properties of Polar Molecules in Crystals. *J. Am. Chem. Soc.* **2015,** *137* (13), 4477-4486.